PROCEEDINGS OF SPIE

SPIEDigitalLibrary.org/conference-proceedings-of-spie

Analytical method for processing digital images of technical objects

Tamara Manko, Iryna Gusarova, Victoria Ogorenko, Ihor Derevianko, Georgiy Lisachuk, et al.

Tamara Manko, Iryna Gusarova, Victoria Ogorenko, Ihor Derevianko, Georgiy Lisachuk, Ruslan Kryvobok, Olena Lapuzina, Andrzej Kotyra, Saule Smailova, "Analytical method for processing digital images of technical objects," Proc. SPIE 10808, Photonics Applications in Astronomy, Communications, Industry, and High-Energy Physics Experiments 2018. 108081C (1 October 2018); doi: 10.1117/12.2501695

SPIE.

Event: Photonics Applications in Astronomy, Communications, Industry, and High-Energy Physics Experiments 2018, 2018, Wilga, Poland

Analytical method for processing digital images of technical objects

Tamara Manko[a], Iryna Gusarova[b], Victoria Ogorenko[c], Ihor Derevianko[d], Georgiy Lisachuk[e], Ruslan Kryvobok*[e], Olena Lapuzina[e], Andrzej Kotyra[f], Saule Smailova[g]
[a]Oles Honchar Dnipro National University, 72 Gagarin Ave., 49010, Dnipro, Ukraine; [b]State Enterprise "Design Bureau" "Yuzhnoye named after M.K. Yangel", 3 Krivorozskaya St., 49008, Dnipro, Ukraine; [c]State Establishment "Dnipropetrovsk Medical Academy of Health Ministry of Ukraine", 9 Vernadsky St., 49000, Dnipro, Ukraine; [d]Yuzhnoye State Design Office, 3 Krivorozskaya St., 49008, Dnipro, Ukraine; [e]National Technical University "Kharkiv Polytechnic Institute", 2, Kyrpychova St., 61002, Kharkiv, Ukraine; [f]Lublin University of Technology, Nadbystrzycka 38a, 20-618 Lublin, Poland; [g]East Kazakhstan State Technical University named after D.Serikbayev, 69 A.K. Protozanov St., 070004 Ust-Kamenogorsk, Kazakhstan

ABSTRACT

The paper presents a method of processing digital images of technical objects whose surfaces are inaccessible. An analytical method of vision data preparation for supporting the decision making about the presence of abnormal areas is presented. The method takes into account the changes of some statistical brightness parameters (intensity, correlation, coordinates, sizes, and shapes) by analyzing matrices of brightness fluctuation, differences (estimates of the rate of brightness changes), variances and correlations, containing information about their state.

Keywords: digital image, mathematical model, statistical processing, state estimation, visual-analytical method

1. INTRODUCTION

The possibilities of assessing the state of technical objects by examining digital images of their surfaces that are not available for measuring instruments of nondestructive testing are considered. Digital images are described by brightness matrices whose measurements $x(i, j)$ are integer samples of auto and mutually correlated random variables of their rows and columns with unknown statistical patterns. The change in these regularities on these or other parts of the surface may contain information on the state of the objects under inspection. Such areas are called textures with their statistical regularities and their parameters. The methods for their investigation and detection are described in [1-5].

Experimental matrices $x(i, j)$ are estimated by mathematical expectations, selective variances, co-variances, empirical laws for the distribution of brightness probabilities (histograms). This knowledge is necessary, but not sufficient for the preparation of data on which decisions can be made about the status of the monitored technical facilities in their design, development, modernization and testing. Textures should be detected; their features and parameters must be determined; and cause-and-effect relationships with assessments of the monitored objects' states should be established.

It is proposed a visual-analytical method of computer processing of experimental matrices of material surfaces digital images' measuring, of the technical objects made of them and data preparation for supporting decision making about their condition.

2. MATHEMATICAL MODELS OF MEASURING DIGITAL IMAGES

The matrix of experimental measurements of the brightness of a digital image $x(i, j)$ of a rectangular surface is considered, where (i, j) are the coordinates of the measurements $i = 1,2,\ldots N_1$ and $j = 1,2,\ldots N_2$. Measurements $x(i, j)$ are integer random variables from 0 to 255 units of brightness, taking these values with probability $p(i, j)$. The tonality of the digital image depends on the values of the probability $p(i, j)$. If $p(i, j) < 0.25$, it corresponds to the dark parts of the image, whereas if $p(i, j) > 0.75$, then the parts are considered as light. Gray areas are characterized by inequality $0.25 \le p(i, j) < 0.75$. If $p(i, j) = 0$, then we have an absolutely black surface and if $p(i, j) = 1$, it is absolutely white surface. In Fig. 1 a digital image of a three-ton surface is shown, where the section at the top is $p(i, j) = 0.25$, the section in the center is $p(i, j) = 0.5$, the section on the bottom is $p(i, j) = 0.75$.

*krivobok_ruslan@ukr.net

Photonics Applications in Astronomy, Communications, Industry, and High-Energy Physics Experiments 2018, edited by Ryszard S. Romaniuk, Maciej Linczuk, Proc. of SPIE Vol. 10808, 108081C
 · doi: 10.1117/12.2501695

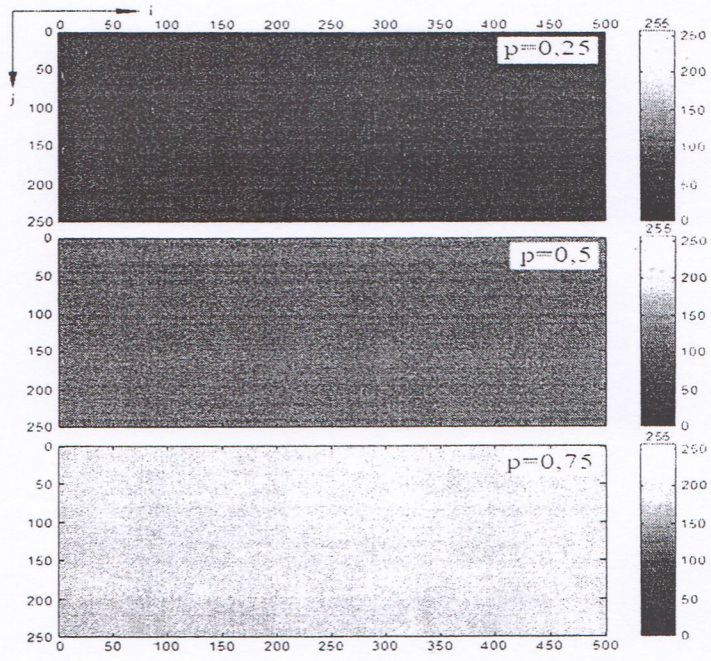

Figure 1. Digital image of a three-ton surface.

If the discrete brightness value 0, 1, ..., 255 is denoted as q, then the probability of the brightness distribution $p(q)$ of a monotone digital image is described by binomial law

$$p(q) = C_n^q p^q (1-p)^{n-q} \tag{1}$$

The mathematical expectation of brightness of the digital image is equal to $M(q) = np$, the dispersion characterizes scattering of brightness relative to $M(q)$ and is equal to $D(q) = np(1-p)$. The total number of random variables of the matrix $x(i, j)$ is $N = N_1 N_2$. The average brightness of the image $\bar{x}$ depends on the probability p. If the matrix $x(i, j)$ is known, then the mean $\bar{x}$ and sample variance $\overline{D}$ can be estimated, and their mathematical expectations $M(\bar{x})$ and $M(\overline{D})$ are equal to

$$\bar{x} = \frac{1}{N}\sum_{i=1}^{N_1}\sum_{j=1}^{N_2} x(i, j), \qquad \overline{D} = \frac{1}{N}\sum_{i=1}^{N_1}\sum_{j=1}^{N_2}(x(i, j) - \bar{x})^2 \qquad M(\bar{x}) = np, \qquad M(\overline{D}) = np(1-p). \tag{2}$$

The binomial law of probability distribution for large values can be approximated by the normal (Gaussian) distribution law

$$p(q) = \exp\left(-\frac{(q-np)^2}{2np(1-p)}\right) \Big/ \sqrt{2\pi np(1-p)} \tag{3}$$

Using (3) and changing the values p, one can simulate matrices of single-tone digital images as sequences of measurements of rows $x(j/i)$ or columns $x(i/j)$ of independent normal random variables of different intensity. Matrices of measurements of real digital images $x(i/j)$ are auto and mutually correlated samples of random measurements of rows $x(j/i)$ and columns $x(i/j)$.

Let's consider a matrix of neighbors $x(i/j)$, where the measurement $x(i/j)$ is statistically related to three neighboring dimensions $x(i, j-1)$, $x(i-1, j)$ and $x(i-1, j-1)$. This relationship can be described by the following equation:

$$x(i, j) = \bar{x} + \left(r_1 x(i, j-1) + r_2 x(i-1, j) - r_1 r_2 x(i-1, j-1) + \sqrt{\overline{D}(1-r_1^2)(1-r_2^2)}\,\xi(i, j)\right) \tag{4}$$

where r_1 and r_2 are correlation coefficients of rows and columns; $\xi(i, j)$ are forming sequence of independent normal random variables with zero mathematical expectation and unit variance, the first row and the first column of the expression (4) are described by the difference Markov equation.

In Fig. 2 the gray digital images $x(i, j)$ with mathematical expectation $M[x(i,j)] = 128$ and variance $D[x(i,j)] = 64$ differing only in correlation coefficients, are shown; while in Fig. 2a the images with the same correlation coefficients $r_1 = r_2$ are shown. In Fig. 2b the images with correlation coefficients that differ $r_1 \neq r_2$ are shown.

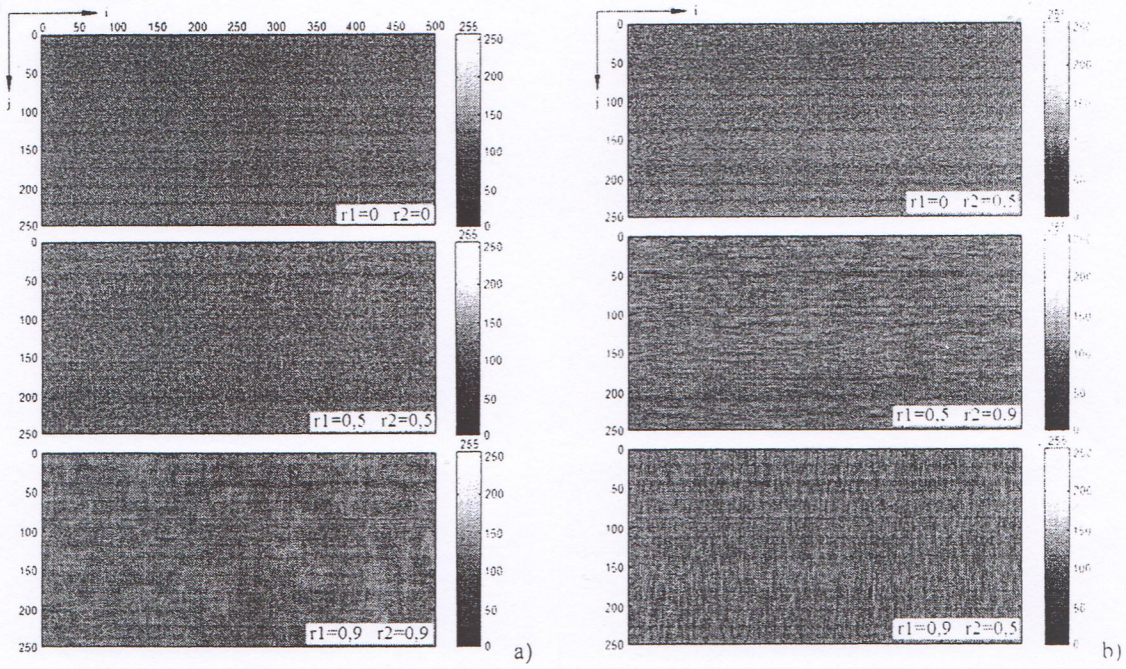

Figure 2. Gray images with correlation coefficients (a) (b).

Mathematical models of textures are areas with altered statistical patterns. The following texture classes can be distinguished:

– areas with changed mathematical expectations of brightness, with changed variances or with changed mathematical expectations and variances, differing in size and shape of the area;
– areas with various changes in correlation relationships or with the destruction of correlations;
– areas with changes in both brightness and correlations;
– changes in certain statistical patterns on the entire surface of the digital image.

3. THE INTEGRAL PARAMETERS' ESTIMATION OF MEASUREMENTS OF EXPERIMENTAL DIGITAL IMAGES' MATRICES

The initial concept of a controlled object surface state can be obtained by evaluating and analyzing the integral parameters of matrices measurements [10]. The mean value of the measurements $\bar{x}$, their sample dispersion $\overline{D}$ by expressions (2) and correlation coefficient

$$\bar{r} = \frac{\sum_{i=2}^{N_1}\sum_{j=2}^{N_2}\frac{1}{3}\Delta x(i,j)\left(\Delta x(i-1,j)+\Delta x(i,j-1)+\Delta x(i-1,j-1)\right)}{(N_1-1)(N_2-1)\overline{D}}, \quad \Delta x(i,j) = x(i,j) - \bar{x} \tag{5}$$

The empirical law of probability distribution of brightness (histogram) and the empirical function of digital images is calculated by the formula:

$$W(q) = F(q) - F(q-1), \quad F(q) = \frac{1}{N'} \sum_{i=1}^{N_1} \sum_{j=1}^{N_2} u(q - x(i,j)), \quad q = 0,1,2,\ldots,255 \tag{6}$$

where $u(z)$ is the unit jump function. If $z \geq 0$, it is equal to 1 and if $z < 0$, it is equal to 0.

$$M[q] = \sum_{q=0}^{255} qW(q) \qquad D[q] = \sum_{q=0}^{255} (q - M[q])^2 W(q)$$
$$K_{sk} = (D[q])^{-\frac{3}{2}} \sum_{q=0}^{255} (q - M[q])^3 \qquad K_{exs} = (D[q])^{-2} \sum_{q=0}^{255} (q - M[q])^4. \tag{7}$$

As an example, in Fig. 3 the empirical laws of probability distribution of digital images brightness for dark $p(i,j) = 0.25$, gray $p(i,j) = 0.5$ and light $p(i,j) = 0.75$ areas are demonstrated. Wherein any changes in the correlation of brightness measurements do not entail their changes. The integral parameters of measurements of digital image matrices, three-tone random surfaces and variously correlated gray $p(i,j) = 0.5$ surfaces are presented in Table 1 and 2, respectively.

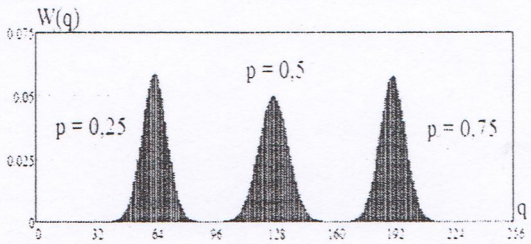

Figure 3. Empirical laws of probability distribution of the digital image brightness.

Table 1. Integral parameters for measuring matrices of digital images of three-ton surfaces.

	p = 0.25 r1 = r2 = 0	p = 0.5 r1 = r2 = 0	p = 0.75 r1 = r2 = 0
$\bar{x}$	64.01	128.01	192.01
$\sqrt{D}$	6.926	7.998	6.926
$\bar{r}$	-0.0006	-0.0005	-0.0006
K_{sk}	0.00252	0.00248	0.00253
K_{exs}	-0.00189	-0.00178	-0.00181

Table 2. Integral parameters for measuring digital image matrices of differently correlated gray surfaces.

	r1=0 r2=0	r1=0.5 r2=0.5	r1=0.9 r2=0.9	r1=0 r2=0.5	r1=0.5 r2=0.9	r1=0 r2=0.9
$\bar{x}$	128.01	127.99	128.04	127.99	127.97	127.98
$\sqrt{D}$	7.998	7.999	7.961	8.009	8.004	8.002
$\bar{r}$	-0.0005	0.417	0.870	0.167	0.617	0.300
K_{sk}	0.00248	-0.00383	-0.00107	0.00052	-0.00368	-0.00207
K_{exs}	-0.00178	-0.00306	0.00107	-0.00562	-0.00440	-0.00269

Histograms and these statistical integral parameters are used for visual observation and control of technical objects to test the hypothesis of their constancy and the absence of texture changes in brightness.

4. TRANSFORMATION AND ANALYSIS OF MEASUREMENT MATRICES OF THE BRIGHTNESS OF DIGITAL IMAGE

The average value of matrix measurements $x(i, j)$ is characterized by radiation sources or reflection of the surface of controlled objects, and fluctuations $\Delta x(i, j) = x(i, j) - \bar{x}$ are the indicators of their reflective or radiative abilities. They contain information about the texture changes in digital image measurements. Fluctuations are also the changes in brightness from the measurement point $(i, j)$to the points $(i, j+1)$ and $(i+1, j)$, i.e., brightness variation on a line and on columns which are characterized their correlations.

We denote the fluctuations as $\Delta x(i, j) = y(i, j)$. Then the rate of their change along the lines is described by the difference $\Delta y(j/i) = y(i, j) - y(i, j-1)$, and by the columns by the difference $\Delta y(i/j) = y(i, j) - y(i-1, j)$. The first differences of rows and columns are mutually perpendicular so that the velocity vectors and directions of measurements of the fluctuation difference $\Delta y(i, j)$and $\varphi(i, j)$are calculated by formulas

$$\Delta y(i, j) = \sqrt{\Delta y^2(j/i) + \Delta y^2(i/j)} \quad \varphi(i, j) = arctg\left(\frac{\Delta y(j/i)}{\Delta y(i/j)}\right) \tag{8}$$

Thus, the brightness fluctuations and the rate of their change are described by the matrices $y(i, j)$, $\Delta y(i, j)$and $\varphi(i, j)$. They contain information about the textures of the brightness of digital image $x(i, j)$. We will carry out their statistical analysis.

First, let's test the hypothesis of the uniformity of a digital image $x(i, j)$.. In this case, the mathematical expectation of the fluctuations $M[y(i, j)]$is uniform. We determine the mean value $\bar{y}^*(i, j)$and variance $D^*[\bar{y}^*(i, j)]$and if in this case the inequality

$$-3\sqrt{\bar{D}^*[\bar{y}^*(i, j)]} \le \bar{y}^*(i, j) \le 3\sqrt{\bar{D}^*[\bar{y}^*(i, j)]} \tag{9}$$

is executed, then the matrix $x(i, j)$ can be regarded as one-ton with a probability of 0.997. In this case the variance of the mean is described by the formula

$$\bar{D}^*[\bar{y}^*(i, j)] = \frac{D^*[\bar{y}^*(i, j)]}{(N_1 - 1)(N_2 - 1)}. \tag{10}$$

The statistical parameters of the fluctuations $y(i, j)$ differ from the measurement matrices $x(i, j)$ only by the mean value. Let us now analyze the velocity and direction vectors for measuring the difference in the fluctuations $\Delta y(i, j)$ and $\varphi(i, j)$. In Fig. 4 the histograms $\Gamma(\Delta y)$ and $\Gamma(\Delta\varphi)$ obtained by processing a gray image with different correlation parameters are shown.

The law of distribution of probabilities of the velocity vector of measurements of the difference of fluctuations $\Delta y(i, j)$ is close to the Rayleigh distribution. In this case, the more correlated the measurements are, the less scatter the values on the histogram is. The law of the vector of direction measurement of the fluctuations' difference $\varphi(i, j)$, depending on the correlation, has a different form.

Obviously, in contrast to the histograms of the initial measurements obtained by the Habibie model, the shape and parameters of the histograms of velocity vectors and of fluctuation difference measurement direction depend strongly on the parameters of measurements' correlation and allow us to obtain useful information for the analysis of textures.

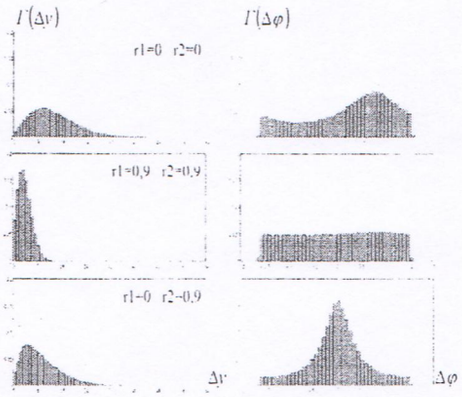

Figure 4. Histograms of the velocity vectors and the direction of measurement of fluctuation differences $I'(\Delta y)$ and $I'(\Delta\varphi)$

Information about textures is also contained in the matrices of the covariance of measurements, which are formed within a moving window in size $(1+\tau)^2$

$$R(i,j)=\frac{\sum_{t=-\tau}^{-1}\Delta x(i,j)\left(\Delta x(i+t,j)+\Delta x(i,j+t)+\Delta x(i+t,j+t)\right)}{3\tau}, \qquad (11)$$

where τ is the shift, i.e., the number of measurements (i,j) adjacent to the investigated point participating in the transformation. Matrices of covariance contain simultaneously information about changes in variances and correlations within the moving window $R(i,j)=\overline{D}(i,j)r(i,j)$.

We perform statistical factor analysis of the matrices of covariance of the 1st ($\tau=1$) and 2nd ($\tau=2$) order from the matrix $x(i,j)$ described by the Habibie equation. The second-order covariance histograms are very similar to the first-order histograms shown above. The differences between them are in their statistical indicators, given in Table 3.

Table 3. Integral parameters of measurements of covariance matrices of the first and second order from the matrix $x(i,j)$.

		r1=0 r2=0	r1=0.5 r2=0.5	r1=0.9 r2=0.9	r1=0 r2=0.5	r1=0 r2=0.9	r1=0.5 r2=0.9
τ = 1	$\overline{R}$	-0.112	26.250	56.638	10.409	19.156	39.605
	$\sqrt{\overline{D}(R)}$	36.462	55.872	87.407	43.443	50.011	68.875
	$K_{sk}(R)$	-0.068	2.411	3.282	1.323	1.959	2.856
	$K_{exs}(R)$	5.619	10.217	17.535	6.920	7.902	12.939
τ = 2	$\overline{R}$	-0.051	19.070	53.496	7.850	17.807	32.138
	$\sqrt{\overline{D}(R)}$	25.956	44.586	83.344	31.872	40.587	60.021
	$K_{sk}(R)$	-0.011	2.438	3.271	1.442	2.596	3.139
	$K_{exs}(R)$	6.199	12.129	17.432	8.020	13.024	16.793

It can be noticed the integral parameters of the measurements of the first and second order covariance matrices depend on the scatter parameters and the correlation of the measurements, as a consequence, can be used for factor analysis of

measurements and allocation of textures. Second-order covariance estimates have a smaller spread, that is, the estimates obtained are more accurate and carry more accurate information about the correlation of the measurements with Yulovsky sequences in measurements' forming according the Habiby model.

5. THE THEORETICAL BASIS FOR THE EVALUATION AND DETECTION OF TEXTURES

Statistical theories of recognition and detection are based on knowledge of the laws of distribution of the probability of measurements or knowledge of samples of objects' measurements in different states [8, 9]. This theoretical knowledge is needed, but it is not enough to solve the problem of detecting texture changes in digital images that are only being designed, developed or modernized.

The main feature of textures is the concentration of measurements with the same parameters (in the statistical sense). This set of measurements-neighbors with almost identical averages, selective variances, correlations, histograms. These are the same fragments of texture matrices that need to be selected from the matrices $x(i, j)$, $\Delta y(i, j)$, $\varphi(i, j)$ and $R(i, j)$, then determine the location of these textures, sizes, shape, intensity and density.

Texture patches can be visually seen by observing digital images. However, we should not forget that the visual examination of images by operators is subjective, since they may have a lack of experience and skills, or be in anxiety, stress and depression, as a result, lose the opportunity to concentrate attention and make the right decisions. The levels of anxiety, stress and depression of operators before each control should be assessed using modern computerized psychometric testing. Therefore, matrixes for measuring digital images should be processed in order to contrast the selection of textures as the support in making decision about operators.

The texture of the monitored object, which is changed on some part of the brightness surface, is shown on the histogram in the form of a second maximum. But the histogram is strongly compressed information about the probability of brightness distribution. With small changes in the statistical parameters of the texture and in small areas, this texture may not change the histogram. Japanese scientist Nobuyuki Otsu proposed a computer technology of testing the hypothesis that a digital image contains measurements of two classes, differing in their brightness and quantity [10,11]. The law of probability distribution of brightness measurements q, as a random variable from 0 to 255 units, in this case is described by expression:

$$W(q) = p_1 W_1(q) + p_2 W_2(q), \quad 0 \le q \le 255, \tag{12}$$

where p_1 and p_2 are probabilities that q refers to either the first or second class; $W_1(q)$ and $W_2(q)$ are unknown laws for the distribution of probabilities of their brightness.

Since $W(q)$ is the known function (6), it is possible to determine the dispersion of brightness measurements as a function of the separation threshold

$$D_{12}(q_n) = p_1(q_n) D_1(q_n) + p_2(q_n) D_2(q_n). \tag{13}$$

If the matrix contains measurements of two classes, then the dispersion relation $D_{12}(q_n)$ from the measurement separation threshold has a minimum $\min(D_{12}(q_n))$ and it can be used as a threshold for dividing the measurements $x(i, j)$ into two classes.

Otsu showed that there is also a dependence of the interclass dispersion on the separation threshold, which is determined by the formula

$$D'_{12}(q_n) = p_1(q_n) p_2(q_n) (M_1(q_n) + M_2(q_n))^2, \tag{14}$$

has a maximum $\max(D'_{12}(q_n))$, and this threshold value can also be used in the problem of classifying measurements of matrices of random variables. By placing a histogram $W(q)$ of the digital image $x(i, j)$ and calculating probabilities and mathematical expectations

$$p_1(q_n) = \sum_{q=0}^{q_n} W(q), \quad p_2(q_n) = 1 - p_1(q_n), \quad M_1[q] = \sum_{q=0}^{q_n} qW(q), \quad M_2[q_n] = \sum_{q=q_n}^{255} qW(q) \tag{15}$$

, it is possible to determine the value q_n, at which the interclass dispersion is maximal. Using the threshold, we'll perform a binary transformation of the measurement matrix $x(i, j)$,

$$B_x(i,j)) = u\left(x(i,j) - q_u\right). \tag{16}$$

This matrix of zeros and ones forms a black and white image, which is examined with the following aim:
– determination of brightness textures exceeding the threshold;
– determination of coordinates, sizes and area of textures;
– selection of matrix textures$\Delta y(i,j)$, $\varphi(i,j)$ and $R(i,j)$.

For example, let's consider a gray digital image $p(i,j) = 0.5$ with correlation $r_1 = r_2 = 0.5$, in which there is an anomalous area with 64 × 64 dimensions, which center is in the coordinate 160 × 154. This part differs only in its correlation $r_1 = r_2 = 0.8$. The results of its statistical processing are shown in Fig. 5, where the digital images of the matrices $x(i,j)$, $\Delta y(i,j)$, $\varphi(i,j)$, $D(i,j)$ and $R(i,j)$ are on the left, and their binary representation are on the right.

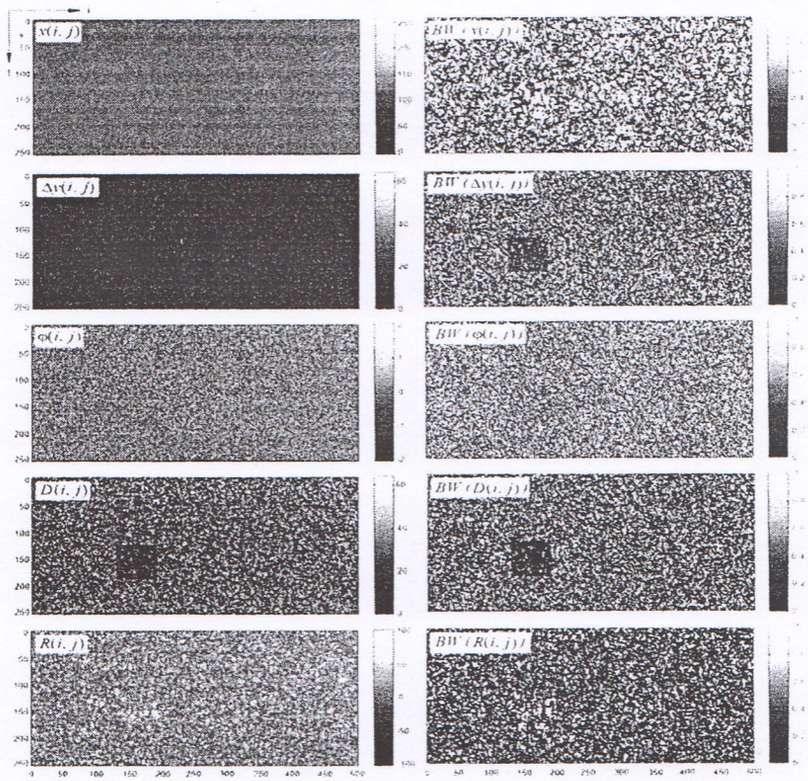

Fig. 5. Digital images of matrices $x(i,j)$, $\Delta y(i,j)$, $\varphi(i,j)$, $D(i,j)$, $R(i,j)$ and their binary representation.

6. THE INTRODUCTION OF METHODS FOR THE EVALUATION AND DETECTION OF TEXTURES IN THE STUDY OF IMAGES OF THE SURFACE OF HEAT-SHIELDING STRUCTURES IN THE RST. EFFICIENCY OF THE METHOD

Currently, one of the priority areas in the development of rocket and space technology is the creation of reusable aircraft, which allow a significant reduction in the cost of bringing cargo into orbit. With the repeated use of complex and expensive equipment operating under extreme conditions, the task of diagnosing its condition becomes particularly acute. One of the most important designs of reusable aircrafts are their external heat-shielding structures, subject to high temperatures and aerodynamic loads when starting and returning products. A 3D model of such a heat-shielding system is shown in Fig. 6

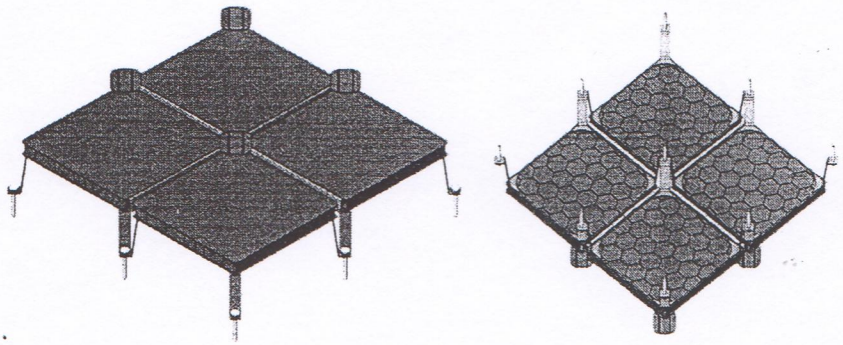

Figure 6. 3D model of heat-shielding system.

The quality control of the thermal protection of reusable aircrafts is carried out with unilateral access to these structures within the apparatus. Therefore, one of the main methods of their control is the assessment of the state of technical objects through visual control of surfaces. But visual control is not enough to make a decision about the state of the object under study and is supplemented by the results of processing measurements of more informative methods: holographic and thermometric. When using these methods, information on the state of the monitored thermal protection structures is contained in digital images of their surface.

As an example, in Fig. 7a the thermographic and holographic measurements of the honeycomb metal panel of the heat-shielding structure are shown. Such measurements were processed using the visual analytical method of processing digital images of technical objects, statistical matrices $x(i,j)$, $\Delta y(i,j)$, $\varphi(i,j)$, $D(i,j)$, $R(i,j)$ and their binary representations were obtained. The results of their analysis of the presence and size of the textures (in this case, defects in the form of impurities) are summarized in the visual defectogram shown in Fig. 7b, on which all the detected defects are brought together.

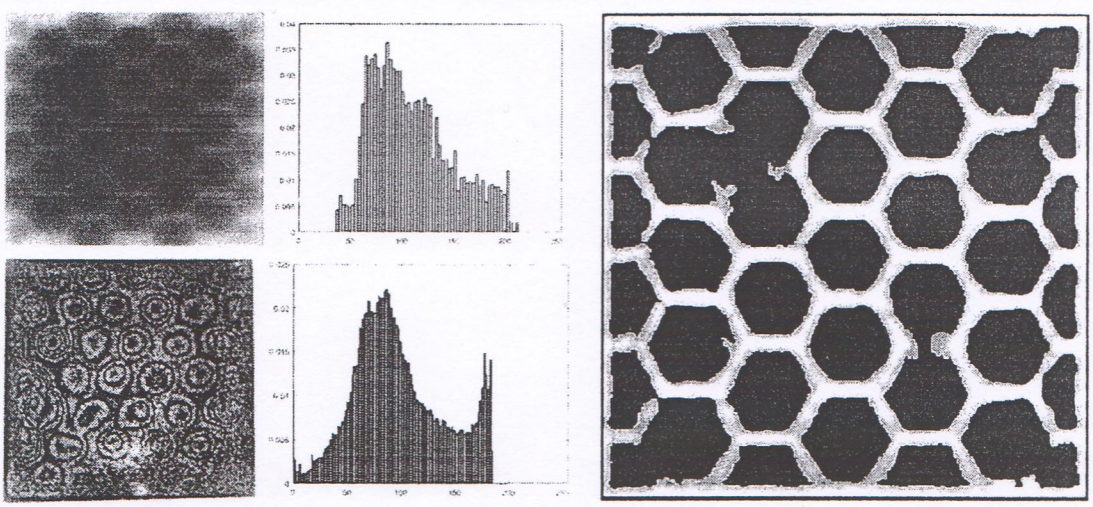

a) b)

Figure 7. Thermographic and holographic measurements (a) and visual defectogram (b) of a cellular metal panel of heat-protective structure.

The efficiency of the visual-analytical method for processing digital images of technical objects η was estimated by the ratio of the area S_{NDT} of textures (defects) from the defectogram, obtained during the processing of measurements of nondestructive testing with the area S_d of real defects, obtained by contact measurement of the non-adhesive places of the cell to the upper skin after removal of the lower skin cellular metal panel.

$$\eta = S_{NDT} / S_d \quad (17)$$

The efficiency η of the visual-analytical method for processing digital images of technical objects in the case of examining the cellular metal panel of the heat-shielding structure shown in Fig. 6, is 0.948. In this case, the probability of defects' detection and the accuracy of determining the geometric dimensions of the method using the results of analysis of all matrices $x(i,j)$, $\Delta y(i,j)$, $\varphi(i,j)$, $D(i,j)$, and $R(i,j)$ is much higher than using the results of analysis of each of the matrices separately.

7. CONCLUSIONS

In the conditions of a lack of prior knowledge about statistical regularities of measuring the brightness of surface digital images of technical facilities being developed that are inaccessible to visual observation and non-destructive testing devices use, the visual-analytical method of preparing data to support decision making about their condition is the most informative.

Changes in the state of technical objects are manifested in changes of statistical regularities' measurements in individual sections of digital images and their detection, estimation of coordinates, dimensions and statistical parameters is the goal of the proposed visual-analytical method.

Digital images, as matrices of experimental brightness measurements, are samples of rows and columns of auto- and mutually correlated normal random variables, with unknown parameters (mathematical expectations, variances, correlations). The sections on them with the changed parameters (textures) can be simple (one-parameter) and complex (two and three-parameter). Information on texture changes is contained in the matrix of brightness fluctuations and in the matrix of the velocity vector of fluctuations' changes of the experimental matrix.

REFERENCES

[1] Tomasi, C., and Manduchi, R., "Bilateral filtering for gray and color images", Proc. IEEE 6th int. Conf. on Computer Vision, 839-846 (1998).

[2] Chochia, P. A., "Image enhancement using sliding histograms", Computer Vision, Graphics, Image processing, 44(2), 211-229 (1988).

[3] Li, S. Z., [Markov random field modeling in image analysis], Springer-Verlag, New York, 1-313 (2009).

[4] Pratt, W. K., [Introduction to Digital Image Processing], CRC Press, Boca Raton, 393-619 (2014).

[5] Lee, J. S., "Digital image smoothing and the sigma filter", Computer vision Graphics Image processing 24(2), 255-269 (1983).

[6] Gonzalez, R. C., and Woods, R. E., [Digital Image Processing, 3rd ed.], Pearson, Upper Saddle River, 1-926 (2010).

[7] T.J. Keating, P.R. Wolf, and F.L. Scarpace "An Improved Method of Digital Image Correlation" Photogrammetric Engineering and Remote Sensing 41(8) 993-1002 (1975).

[8] Ackermann, F. "Digital image correlation: Performance and potential application in photogrammetry", Photogrammetric Record, 11(64) 429-439 (1984).

[9] Maybeck, P. S., [Stochastic models, estimation, and control], Academic Press, New York, 1-424 (1979).

[10] Vala, H. J., and Baxi, A. "A review on Otsu image segmentation algorithm", International Journal of Advanced Research in Computer Engineering & Technology (IJARCET) 2(2), 387-389 (2013).

[11] Sezgin, M., and Sankur, B., "Survey over image thresholding techniques and quantitative performance evaluation", Journal of Electronic Imaging, 13(1), 146-165 (2004).

[12] Antonenko, Y. A., Mustetsov, T. N., Hamdi, R. R., Malecka-Massalska, T., Orshubekov, N., Dzierzak, and R., Uvaysova, S., "Double-compression method for biomedical images," Proc. of SPIE 10445, (2017).

[13] Kaczmarek, C., and Wójcik, W., "Measurement of pressure sensitivity of modal birefringence of birefringent optical fibers using a Sagnac interferometer", Optica Applicata 45(1), 5-14 (2015).

[14] Maciejewski, M., Surtel, W., Wójcik, W., Masiak, J., Dzida, G., and Horoch, A., "Telemedical systems for home monitoring of patients with chronic conditions in rural environment", Annals of Agricultural and Environmental Medicine 21(1), 167-173 (2014).

[15] Grudzień, K., and Sankowski, D., "Methods for monitoring gravitational flow in silos using tomography image processing", IAPGOŚ 7(1), 24-29 (2017).